HEAT CONDUCTION IN CONVECTIVELY COOLED ECCENTRIC SPHERICAL ANNULI
A Boundary Integral Moment Method

by

Ayhan YILMAZER [*] ***and Cemil KOCAR***

[a]Department of Nuclear Engineering, Hacettepe University, Beytepe, Ankara, Turkey

Original scientific paper1
https://doi.org/10.2298/TSCI151231128Y

In this paper heat conduction equation for an eccentric spherical annulus with the inner surface kept at a constant temperature and the outer surface subjected to convection is solved analytically. Eccentric problem domain is first transformed into a concentric domain via formulating the problem in bispherical co-ordinate system. Since an analytical Green's function for the heat conduction equation in bispherical co-ordinate for an eccentric sphere subject to boundary condition of third type can not be found, an analytical Green's function obtained for Dirichlet boundary condition is employed in the solution. Utilizing this Green's function yields a boundary integral equation for the unknown normal derivative of the surface temperature distribution. The resulting boundary integral equation is solved analytically using method of moments. The method has been applied to heat generating eccentric spherical annuli and results are compared to the simulation results of FLUENT CFD code. A very good agreement was observed in temperature distribution computations for various geometrical configurations and a wide range of Biot number. Variation of heat dissipation with radii and eccentricity ratios are studied and a very good agreement with FLUENT has been observed.

Keywords: *eccentric sphere, heat conduction, boundary integral equation, Green's function*

Introduction

Heat conduction in a concentric spherical annulus with or without heat generation is the subject of standard heat transfer textbooks and well developed. Interested readers may refer to the textbook by Ozisik [1] for the analytical solutions of linear heat conduction equation for concentric spherical annuli exposed to uniform boundary conditions of any kind and any functional form of space dependent heat generation rate. However, solving conduction equation analytically for an eccentric spherical annulus has inherent difficulties associated with employing a boundary fitting co-ordinate system and application of boundary conditions. Bispherical co-ordinate is a convenient orthogonal co-ordinate system which fits both boundaries of an eccentric spherical annulus and allows application of first type boundary conditions directly. For example, conduction equation for two adjacent spheres without heat generation located at any distance from each other was solved analytically by Alassar and Alminshawy [2] in bispherical co-ordinate. They solved steady-state axisymmetric heat conduction equation for two isothermal spheres at different temperatures (first type boundary conditions) with different radii.

[*]Corresponding author, e-mail: yilmazer@hacettepe.edu.tr

Alassar [3] solved the conduction equation analytically for an eccentric spherical annulus with first type boundary conditions and uniform heat generation rate. The solution was the superposition of solutions in bispherical co-ordinate of R-separable Laplace equation and a particular solution. It was limited to the azimuthally symmetrical 2-D problems and to the uniform heat generation rate and could not be applied to a general spatially varying heat generated 3-D eccentric annuli. Since Helmholtz differential equation is not separable or R-separable in bispherical co-ordinate system [4] the conduction equation could not be solved for an eccentric spherical annulus with heat generation in bispherical co-ordinate using standard techniques such as eigenfunction expansion or related methods. Yilmazer and Kocar [5] obtained an exact solution using Green's function method to the 3-D conduction equation through an eccentric spherical annulus with constant surface temperatures and with space dependent heat generation.

While there are several studies as previously illustrated on heat conduction through concentric and eccentric spheres, a literature survey reveals that there is not an exact solution to the conduction equation in a spherical annulus cooled convectively (third type boundary condition) at one or two boundaries. In a recent paper, the authors of this paper developed a new analytical approach based on Green's function method to arrive at a boundary integral equation (BIE) for 2-D steady heat conduction equation in an eccentric cylindrical annulus whose inner boundary was isothermal and outer boundary was subjected to convection [6]. Since an analytical Green's function to the conduction equation in bipolar co-ordinate for an eccentric cylindrical annulus subject to boundary condition of third type could not be found, the problem was treated as a second type boundary value problem. The method is based on developing a BIE in bipolar co-ordinate for the outer surface temperature distribution using the analytical Green's function obtained for second type boundary condition. The resulting BIE was solved by method of moments, referred to as boundary integral moment method (BIMM), producing very accurate results.

In this study BIMM is applied in bispherical co-ordinate to solve heat conduction equation analytically in heat generating 3-D eccentric spherical annuli whose inner surface is kept at a constant temperature and outer surface is subjected to the convection. Instead of treating the problem as a second type boundary value problem as in previous cylindrical annulus conduction problem [6], the eccentric spherical annulus conduction problem is handled as a first type boundary value problem yielding a BIE for the unknown normal derivative of outer boundary temperature which is solved by the method of moments. The BIMM solution proposed in this study which is based on Green's function approach introduces an unknown BIE for the normal derivative of the surface temperature making analytical solution much more involved. The method is applied for a wide range of heat generation ranges and Biot numbers and for various geometrical configurations, *i. e*., eccentricity and radii ratios. The results of temperature distribution and heat transfer calculations are compared with the simulation results obtained from CFD code FLUENT [7].

Definition of the problem

Consider an eccentric spherical annulus with inner surface kept isothermal at temperature T_i and outer surface cooled convectively by a coolant at an ambient temperature, T_∞. Steady-state heat conduction equation for the annulus is:

$$\nabla^2 T + \frac{\dot{q}}{k} = 0 \tag{1a}$$

$$T = T_i \text{ on the inner surface} \tag{1b}$$

$$-k\frac{\partial T}{\partial n} = h(T - T_\infty) \text{ on the outer surface} \tag{1c}$$

where ∇^2 is the Laplacian, $\dot{q}$ [$\mathrm{Wm^{-3}}$] – the volumetric heat generation rate, k [$\mathrm{Wm^{-1}K^{-1}}$] – the thermal conductivity, h [$\mathrm{Wm^{-2}K^{-1}}$] – the convection coefficient, n – the outward normal, and T_∞ [K] – the ambient coolant temperature. Among the known orthogonal co-ordinate systems it is the bispherical co-ordinate for which it is possible to express both boundaries of the eccentric annulus with only one co-ordinate parameter [4, 8, 9].

If radii of the inner and outer spheres are denoted by r_i and r_o, respectively, and center to center distance or eccentricity by e then a bispherical co-ordinate system could be specified by using eq. (3) corresponding to two eccentric constant, ξ, spheres lying along the z-axis:

$$\xi_i = \sinh^{-1}\frac{a}{r_i} \quad \text{and} \quad \xi_o = \sinh^{-1}\frac{a}{r_o} \tag{2}$$

where

$$a = \frac{\sqrt{(e + r_i + r_o)(e + r_i - r_o)(e - r_i + r_o)(e - r_i - r_o)}}{2e} \tag{3}$$

The conduction problem defined by eq. (1) for the convectively cooled eccentric annulus could be expressed in bispherical co-ordinate system:

$$\frac{1}{\bar{h}_\xi^3}\left[\frac{\partial}{\partial\xi}\left(\bar{h}_\xi\frac{\partial}{\partial\xi}\right) + \frac{1}{\sin\theta}\frac{\partial}{\partial\theta}\left(\bar{h}_\xi\sin\theta\frac{\partial}{\partial\theta}\right) + \frac{\bar{h}_\xi}{\sin^2\theta}\frac{\partial^2}{\partial\phi^2}\right]\Psi(\xi,\theta,\phi) + Q(\xi,\theta,\phi) = 0 \tag{4a}$$

with the dimensionless boundary conditions:

$$\Psi(\xi,\theta,\phi) = 1 \quad \text{at} \quad \xi = \xi_i \tag{4b}$$

$$\frac{\partial\Psi(\xi,\theta,\phi)}{\partial\bar{n}} = -\mathrm{Bi}\frac{a}{r_o}\Psi(\xi,\theta,\phi) \quad \text{at} \quad \xi = \xi_o \tag{4c}$$

where Biot number is defined as $\mathrm{Bi} = hr_o/k$ and

$$\bar{h}_\theta = \bar{h}_\xi = \frac{h_\xi}{a} = \frac{1}{\cosh\xi - \cos\theta}, \qquad \bar{h}_\phi = \frac{h_\phi}{a} = \frac{\sin\theta}{\cosh\xi - \cos\theta} \tag{5}$$

are normalized scale factors of the bispherical co-ordinate system.

The BIMM solution

If the inner and outer surfaces of the annulus are denoted by ∂S_i and ∂S_o then the dimensionless conduction equation defined by eq. (12) has the following Green's function solution:

$$\Psi(\xi,\theta,\phi) = \int_{V'} Q'G\mathrm{d}\bar{V}' + \int_{\partial S_i'}\left(G\frac{\partial\Psi}{\partial\bar{n}'} - \Psi\frac{\partial G}{\partial\bar{n}'}\right)\mathrm{d}\bar{S}' + \int_{\partial S_o'}\left(G\frac{\partial\Psi}{\partial\bar{n}'} - \Psi\frac{\partial G}{\partial\bar{n}'}\right)\mathrm{d}\bar{S}' \tag{6}$$

where $G = G(\vec{\mathrm{r}} / \vec{\mathrm{r}}') = G(\xi,\theta,\phi / \xi',\theta',\phi')$ is the Green's function and the prime shows the computational domain. Green's function satisfies the following equations:

$$\frac{1}{\overline{h}_\xi^3}\left[\frac{\partial}{\partial\xi}\left(\overline{h}_\xi\frac{\partial}{\partial\xi}\right)+\frac{1}{\sin\theta}\frac{\partial}{\partial\theta}\left(\overline{h}_\xi\sin\theta\frac{\partial}{\partial\theta}\right)+\frac{\overline{h}_\xi}{\sin^2\theta}\frac{\partial^2}{\partial\phi^2}\right]G(\vec{\mathrm{r}} / \vec{\mathrm{r}}')+\delta(\vec{\mathrm{r}}-\vec{\mathrm{r}}')=0 \tag{7a}$$

$$G\left(\xi,\theta,\phi / \xi',\theta',\phi'\right)=0 \quad \text{at} \quad \xi=\xi_i \tag{7b}$$

$$\frac{\partial G\left(\xi,\theta,\phi / \xi',\theta',\phi'\right)}{\partial\overline{n}}=-\mathrm{Bi}\frac{a}{r_o}G\left(\xi,\theta,\phi / \xi',\theta',\phi'\right) \quad \text{at} \quad \xi=\xi_o \tag{7c}$$

where Dirac's delta function could be expressed in bispherical co-ordinate:

$$\delta(\vec{\mathrm{r}}-\vec{\mathrm{r}}')=\frac{\delta(\xi-\xi')\delta(\theta-\theta')\delta(\phi-\phi')}{\overline{h}_\xi\overline{h}_\theta\overline{h}_\phi}=\frac{\delta(\xi-\xi')}{\overline{h}_\xi\overline{h}_\theta\overline{h}_\phi}\sum_{\ell=0}^{\infty}\sum_{m=-\ell}^{\ell}Y_\ell^{m*}(\theta,\phi)Y_\ell^m(\theta',\phi') \tag{8}$$

Since Helmholtz equation in bispherical co-ordinate is neither separable nor R-separable [4], it is not possible to find an analytical expression in bispherical co-ordinate for the Green's function of an eccentric spherical annulus with boundary condition of third kind, *i. e.* convective boundary condition in our problem. However, the original problem described by eq. (7) with third type boundary condition could be transformed into a problem with a first type boundary condition:

$$\frac{1}{\overline{h}_\xi^3}\left[\frac{\partial}{\partial\xi}\left(\overline{h}_\xi\frac{\partial}{\partial\xi}\right)+\frac{1}{\sin\theta}\frac{\partial}{\partial\theta}\left(\overline{h}_\xi\sin\theta\frac{\partial}{\partial\theta}\right)+\frac{\overline{h}_\xi}{\sin^2\theta}\frac{\partial^2}{\partial\phi^2}\right]\Psi(\xi,\theta,\phi)+Q(\xi,\theta,\phi)=0 \tag{9a}$$

with dimensionless boundary conditions:

$$\Psi(\xi,\theta,\phi)=1 \quad \text{at} \quad \xi=\xi_i \tag{9b}$$

$$\Psi(\xi,\theta,\phi)=-\frac{r_o}{a\mathrm{Bi}}\frac{\partial\Psi(\xi,\theta,\phi)}{\partial n}=\frac{r_o}{a\mathrm{Bi}}\frac{1}{\overline{h}_\xi}\frac{\partial\Psi(\xi,\theta,\phi)}{\partial\xi}\bigg|_{\xi=\xi_o} \quad \text{at } \xi=\xi_o \tag{9c}$$

where the normal derivative of the temperature distribution $-\overline{h}_\xi^{-1}\partial\Psi(\xi,\theta,\phi)/\partial\xi\big|_{\xi=\xi_o}$ on the outer boundary is assumed to be known as a priori. Similarly, Green's function satisfies:

$$\frac{1}{\overline{h}_\xi^3}\left[\frac{\partial}{\partial\xi}\left(\overline{h}_\xi\frac{\partial}{\partial\xi}\right)+\frac{1}{\sin\theta}\frac{\partial}{\partial\theta}\left(\overline{h}_\xi\sin\theta\frac{\partial}{\partial\theta}\right)+\frac{\overline{h}_\xi}{\sin^2\theta}\frac{\partial^2}{\partial\phi^2}\right]G(\vec{\mathrm{r}} / \vec{\mathrm{r}}')+\delta(\vec{\mathrm{r}}-\vec{\mathrm{r}}')=0 \tag{10a}$$

$$G\left(\xi,\theta,\phi / \xi',\theta',\phi'\right)=0 \quad \text{at} \quad \xi=\xi_i \tag{10b}$$

$$G\left(\xi,\theta,\phi / \xi',\theta',\phi'\right)=0 \quad \text{at} \quad \xi=\xi_o \tag{10c}$$

Green's function described by eqs. (10) for eccentric spheres in bispherical co-ordinate is derived in [5, 10]:

$$G\left(\xi,\theta,\phi / \xi',\theta',\phi'\right)=\sqrt{\cosh\xi'-\cos\theta'}\sqrt{\cosh\xi-\cos\theta}\sum_{\ell=0}^{\infty}\sum_{m=-\ell}^{\ell}Y_\ell^{m*}(\theta,\phi)Y_\ell^m(\theta',\phi')g_\ell(\xi,\xi') \tag{11a}$$

where Y_ℓ^m are spherical harmonics functions and Y_ℓ^{m*} is the complex conjugate of Y_ℓ^m and $g_\ell(\xi,\xi')$ is the radial part of the Green's function given by:

$$g_\ell(\xi,\xi') = \begin{cases} g_\ell^1(\xi,\xi') = \dfrac{2\sinh\left[\left(\ell+\dfrac{1}{2}\right)(\xi'-\xi_i)\right]\sinh\left[\left(\ell+\dfrac{1}{2}\right)(\xi-\xi_o)\right]}{(2\ell+1)\sinh\left[\left(\ell+\dfrac{1}{2}\right)(\xi_o-\xi_i)\right]} & ,\ \xi<\xi' \\ g_\ell^2(\xi,\xi') = \dfrac{2\sinh\left[\left(\ell+\dfrac{1}{2}\right)(\xi-\xi_i)\right]\sinh\left[\left(\ell+\dfrac{1}{2}\right)(\xi'-\xi_o)\right]}{(2\ell+1)\sinh\left[\left(\ell+\dfrac{1}{2}\right)(\xi_o-\xi_i)\right]} & ,\ \xi>\xi' \end{cases} \tag{11b}$$

It should be noted the factor a in the denominator of $g_\ell^1(\xi,\xi')$ and $g_\ell^2(\xi,\xi')$ in [5] is dismissed in eq. (11b). Because the scale factors are normalized by factor a in the present discussion distinctly from the derivation in [5]. Introducing Green's function given by eqs. (11) and boundary conditions (9b), (9c), (10b), and (10c) into eq. (6) we get:

$$\Psi(\xi,\theta,\phi) = S(\xi,\theta,\phi) - \sqrt{2}\sqrt{\cosh\xi-\cos\theta}\sum_{\ell=0}^{\infty}P_\ell(\cos\theta)\frac{\sinh\left[\left(\ell+\dfrac{1}{2}\right)(\xi-\xi_o)\right]}{\sinh\left[\left(\ell+\dfrac{1}{2}\right)\xi_o-\xi_i)\right]}e^{-(\ell+0.5)\xi_i} +$$

$$+\frac{r_o}{a\mathrm{Bi}}\sqrt{\cosh\xi-\cos\theta}\sum_{\ell=0}^{\infty}\sum_{m=-\ell}^{\ell}\phi_{\ell,m}\frac{\sinh\left[\left(\ell+\dfrac{1}{2}\right)\xi-\xi_i)\right]}{\sinh\left[\left(\ell+\dfrac{1}{2}\right)\xi_o-\xi_i)\right]}Y_\ell^{m*}(\theta,\phi) \tag{12a}$$

where we denoted:

$$\int_{V'} Q'G\,\mathrm{d}\overline{V}' = S(\xi,\theta,\phi) \tag{12b}$$

and the moments $\phi_{\ell,m}$ are defined:

$$\phi_{\ell,m} = \int_0^{2\pi}\int_0^{\pi}\left.\frac{\partial\Psi(\xi',\theta',\phi')}{\partial\xi'}\right|_{\xi'=\xi_o}\sqrt{\cosh\xi_o-\cos\theta'}\sin\theta' Y_\ell^m(\theta',\phi')\,\mathrm{d}\theta'\,\mathrm{d}\phi' \tag{12c}$$

Taking moment of both sides of eq. (12a) by operating:

$$\int_0^{2\pi}\int_0^{\pi}\left.\frac{\partial(.)}{\partial\xi'}\right|_{\xi'=\xi_o}\sqrt{\cosh\xi_o-\cos\theta'}\sin\theta' Y_\ell^m(\theta',\phi')\,\mathrm{d}\theta'\,\mathrm{d}\phi' \tag{13}$$

a linear sytem of infinite number of unknown moments $\phi_{\ell,m}$ could be obtained. Truncating the series solution as $\ell=0,1,2,...,L$ and $m=-\ell,-\ell+1,...-1,0,1,...,\ell-1,\ell$ for the dimensionless temperature given by eq. (12a), this linear system becomes:

$$\sum_{\ell=0}^{L}\sum_{m=-\ell}^{\ell}\phi_{\ell,m}\left[\delta_{\ell',\ell}\delta_{m',m}\left(1-\frac{r_o\sinh\xi_o}{2a\mathrm{Bi}}\right)-\right.$$

$$\left.-\frac{r_o}{a\mathrm{Bi}}\frac{\left(\ell+\frac{1}{2}\right)\cosh\left[\left(\ell+\frac{1}{2}\right)\xi_o-\xi_i)\right]}{\sinh\left[\left(\ell+\frac{1}{2}\right)(\xi_o-\xi_i)\right]}\left(\cosh\xi_o\delta_{\ell,\ell'}\delta_{m,m'}+(-1)^{m+1}2\sqrt{\frac{\pi}{3}}I_{\ell,\ell'}^{-m,m'}\right)\right]=$$

$$=S_{\ell',m'}-\sum_{\ell=0}^{\infty}\frac{\sqrt{2\pi(2\ell+1)}}{\sinh\left[\left(\ell+\frac{1}{2}\right)(\xi_o-\xi_i)\right]}e^{-(\ell+1/2)\xi_i}\left(\cosh\xi_o\delta_{\ell,\ell'}\delta_{0,m'}-2\sqrt{\frac{\pi}{3}}I_{\ell,\ell'}^{0,m'}\right) \tag{14}$$

where $\ell'=0,1,2,...,\ell$ and $m'=-\ell',-\ell'+1,...,0,...\ell'-1,\ell'$. Here, $I_{\ell,\ell'}^{-m,m'}$ and $I_{\ell,\ell'}^{0,m'}$ are integrals involving triple products of spherical harmonics functions and they could be calculated from [8]:

$$\int_0^{2\pi}\int_0^{\pi}Y_{\ell_1}^{m_1}(\theta,\phi)Y_{\ell_2}^{m_2}(\theta,\phi)Y_{\ell_3}^{m_3}(\theta,\phi)\sin\theta\,\mathrm{d}\theta\mathrm{d}\phi=$$

$$=\sqrt{\frac{(2\ell_1+1)(2\ell_2+1)(2\ell_3+1)}{4\pi}}\begin{pmatrix}\ell_1 & \ell_2 & \ell_3\\ 0 & 0 & 0\end{pmatrix}\begin{pmatrix}\ell_1 & \ell_2 & \ell_3\\ m_1 & m_2 & m_3\end{pmatrix} \tag{15}$$

where

$$\begin{pmatrix}\ell_1 & \ell_2 & \ell_3\\ m_1 & m_2 & m_3\end{pmatrix}$$

is Wigner 3-j symbol. Using eqs. (12b) and (13) the moments $S_{\ell',m'}$ could more explicitly be expressed for a given dimensionless heat generation rate distribution $Q(\xi',\theta',\phi')$:

$$S_{\ell',m'}=\sum_{\ell=0}^{\infty}\sum_{m=-\ell}^{\ell}\left\{\frac{1}{2}h_\ell^m(\xi_o)\delta_{\ell,\ell'}\delta_{m,m'}+h_\ell^{m'}(\xi_o)\left(\cosh\xi_o\delta_{\ell,\ell'}\delta_{m,m'}+(-1)^{m+1}2\sqrt{\frac{\pi}{3}}I_{\ell,\ell'}^{-m,m'}\right)\right\} \tag{16a}$$

where

$$h_\ell^m(\xi)=\int_0^{2\pi}\int_0^{\pi}\int_{\xi_o}^{\xi_i}\frac{Q(\xi',\theta',\phi')}{(\cosh\xi'-\cos\theta')^{5/2}}\sin\theta'Y_\ell^m(\theta',\phi')g_\ell(\xi,\xi')\mathrm{d}\xi'\mathrm{d}\theta'\mathrm{d}\phi' \tag{16b}$$

Heat transfer rate

Let us define as in [5] the following dimensionless heat transfer rate:

$$\bar{Q}=\frac{\int_{S_o}h(T-T_\infty)\mathrm{d}S}{k(4\pi r_0^2)\left(\frac{T_i-T_\infty}{r_0}\right)}=\left(\frac{a^2}{4\pi r_0^2}\right)\mathrm{Bi}\left(\int_0^{2\pi}\int_0^{\pi}\Psi\bar{h}_\theta\bar{h}_\phi\mathrm{d}\theta\mathrm{d}\phi\right)\Bigg|_{\xi=\xi_o} \tag{17}$$

Introducing the expression for Ψ given by eq. (12a) into eq. (17), $\bar{Q}$ becomes:

$$\bar{Q}=\frac{1}{\sqrt{2\pi}}\sum_{\ell=0}^{\infty}\sqrt{2\ell+1}e^{-(\ell+1/2)\xi_o}\left[\phi_{\ell,0}+\frac{a\mathrm{Bi}}{r_0}h_\ell^0(\xi_o)\right] \tag{18}$$

where the moments $\phi_{\ell,0}$ are obtained from the solution of the linear system given by eq. (14) and $h_\ell^0(\xi_o)$ is calculated from the expression given by eq. (16b).

An application for uniform source distribution

In this section, the method developed is applied for uniform source distribution. Temperature distributions and dimensionless heat transfer rates for various dimensionless source strengths and a wide range of Biot number are calculated. Comparisons of the analytical results are made with the simulation results of CFD code FLUENT.

The FLUENT was used to solve energy conservation equation in 3-D domain by a second order discretization scheme. In the first sequence of computations, radii ratio is fixed as r_o/r_i = 5.0 and eccentricity ratio is changed as e/r_i =1.0, 2.0, and 3.0, respectively. The residual is set as $1\cdot10^{-11}$ for energy equation. Computational domain is discretized with the mesh numbers 207000, 250000, and 290000 for e/r_i = 1.0, 2.0, 3.0, and 4.0, respectively. In the second set of computations, eccentricity ratio is fixed as e/r_i = 0.5 and radii ratio is changed as, r_o/r_i = 2.0, 3.0, 4.0, and 5.0, respectively. Computational domain is discretized with the mesh numbers 157000, 221000, 425000, 730000 for r_o/r_i = 2.0, 3.0, 4.0, and 5.0, respectively. The quadrilateral mesh elements were used for all the cases. The inner boundary is set as constant temperature boundary while convective boundary condition is applied at outer boundary. The numerical value of the heat transfer coefficient is derived from the Biot number of the interested case. The CFD calculations are done on an AMD 3.0 GHz computer having a 4 GB memory. Decrease in the Biot number and increase in the absolute value of the heat generation resulted in increase of simulation time and number of iterations.

Temperature distribution

The dimensionless temperature distribution in the eccentric sphere for a space dependent source distribution is expressed by eq. (12a). For a constant dimensionless heat generation rate Q, the $S(\xi,\theta,\phi)$ defined by eq. (12b) could be calculated:

$$S(\xi,\theta,\phi)=\sqrt{\cosh\xi-\cos\theta}\sum_{\ell=0}^{\infty}\sum_{m=-\ell}^{\ell}Y_\ell^{m*}(\theta,\phi)h_\ell^m(\xi) \tag{19}$$

where the function $h_\ell^m(\xi)$ defined by eq. (16b) is obtained:

$$h_\ell^m(\xi)=\frac{4Q\sqrt{2\pi(2\ell+1)}}{3}\delta_{m,0}\cdot \frac{e^{-(\ell+1/2)\xi_o}(\coth\xi_o-\coth\xi)\sinh\left[\left(\ell+\frac{1}{2}\right)(\xi-\xi_i)\right]+e^{-(\ell+1/2)\xi_i}(\coth\xi-\coth\xi_i)\sinh\left[\left(\ell+\frac{1}{2}\right)(\xi-\xi_o)\right]}{2\sinh\left[\left(\ell+\frac{1}{2}\right)(\xi_o-\xi_i)\right]} \tag{20}$$

The unknown moments $\phi_{\ell,m}$ in eq. (12a) could be found by solving the linear system of equations given by eqs. (14)-(16) in which the function $h_\ell^m(\xi)$ takes the form specified by eq. (20) for uniform heat generation and this completes the solution.

Effect of source strength on temperature distribution

It is first aimed at observing the effect of source strength on temperature distribution. For this purpose temperature distribution is calculated along the centerline [AB] on yz-plane of outer sphere as shown in fig. 1. Variation of temperature along the line [AB] is depicted in

fig. 2 for various constant heat generation rates: $Q = -50, -25, 0, 25$, and 50 for a geometrical configuration $r_o/r_i = 5.0$ and $e/r_i = 2.0$. The y co-ordinate along the [AB] line which extends from $(0,-r_o, a\coth\xi_o)$ to $(0,r_o, a\coth\xi_o)$ is non-dimensionalized as $y^* = y/(|AB|/2)$ where y^* extends from –1 to 1. It should be noted that r_i, r_o, and e do not define the geometrical configuration themselves. Instead the radii ratio r_o/r_i and eccentricity ratio e/r_i are the parameters identifying geometrical configuration. Namely, irrespective of the values of r_o, r_i and e, dimensionless temperature is merely a function of these dimensionless ratios. Biot number is assigned as 5.0 in all cases. Perfect agreement with CFD results are observed in all computations. The dips in the temperature observed at the middle of [AB] for every heat generation rate is because of isothermal boundary condition exposed on the inner surface of the annulus, *i. e*., unit dimensionless temperature. Symmetrical temperature distributions are observed on both sides of the middle point O_1 where heat generation spans comparatively larger volumes than the lateral sides yielding local maxima on both sides of O_1. As noticed from fig. 2, similar symmetrical like distribution occurs in terms of source strengths with different parities, namely, $Q = \pm$constant. Slight deviation from the symmetry arises from the additive contribution of the inner boundary condition to the temperature distribution for heat source case $Q > 0$. On the contrary, this boundary condition plays an decreasing role on the absolute value of the dimensionless temperature for heat sink cases $Q < 0$.

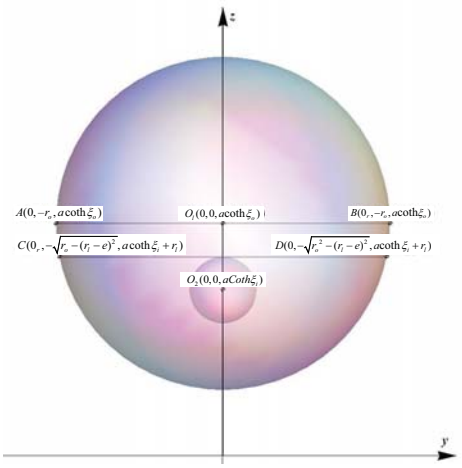

Figure 1. The lines [AB] and [CD] through which dimensionless temperatures are plotted

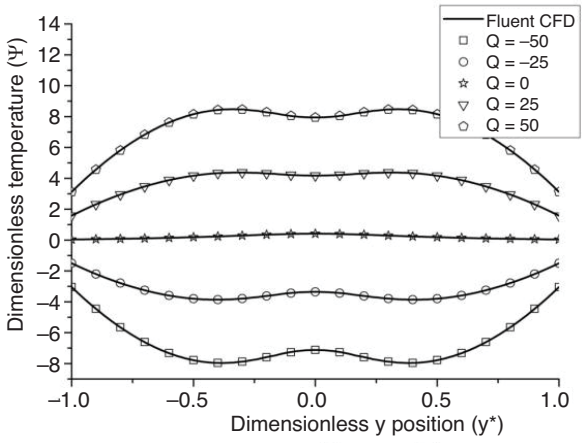

Figure 2. Variation of the dimensionless temperature along the line [AB] by dimensionless position y^* for various dimensionless heat generation rates ($r_o/r_i = 5$, $e/r_i = 2$, Bi = 5.0)

Effect of Biot number on temperature distribution

Figure 3 shows how temperature distribution varies along the line [AB] for various values of Biot number as Bi = 5, 10, 15, and 50. Geometrical configuration for all Biot numbers is kept as $r_o/r_i = 5.0$, $e/r_i = 2.0$ and dimensionless heat generation rate is chosen as $Q = 50.0$. It could be noticed from fig. 3 that for the higher Biot numbers the more effective cooling is observed and lower temperature values are obtained throughout the line [AB] as expected. It could also be noticed from fig. 3 that there exists a complete consistency between BIMM and CFD results.

Effect of eccentricity on temperature distribution

To evaluate the effect of eccentricity on temperature distribution, radii ratio is set at r_o/r_i = 5.0 and various eccentricity ratios as e/r_i = 1.0, 2.0, 2.5, and 3.0 are used in computations. Dimensionless heat generation rate is chosen as Q = 50.0. Variation of temperature distribution along the line [AB] is depicted in fig. 4. As seen from the fig. 4 BIMM results and CFD results are in a very good agreement. It could be noticed from the figure that as the eccentricity is increased the effect of inner boundary condition on temperature distribution along the line [AB] diminishes since inner boundary of the annulus becomes more and more separated from the centerline [AB]. Hence, the governing factor turns out to be the dimensionless heat generation rate not the inner boundary condition for larger eccentricities. When eccentricity is increased high temperature sites become more widespread since a relatively larger heat generating volume in the upper part is formed where total heat generation rate is comparably larger than more concentric cases. It should also be stated that the crescent geometrical configuration ($e = r_o - r_i$) does not yield in convergent results, since the two foci used to describe co-ordinate in bispherical co-ordinate system overlap in this case.

Effect of radii ratio on temperature distribution

In this part, eccentricity ratio is fixed at e/r_i = 0.5 to evaluate the effect of radii ratio on temperature distribution. For this purpose, computations are done for the radii ratios r_o/r_i = 2.0, 3.0, 4.0, and 5.0 with Q = 50.0 and Bi = 5.0. Temperature distribution along the line [CD] is shown in fig. 5 for various radii ratios selected. It could be seen from the fig. 5 that BIMM results and CFD results agree very well. Since the line [CD] is tangent to the top of the inner boundary of the annulus

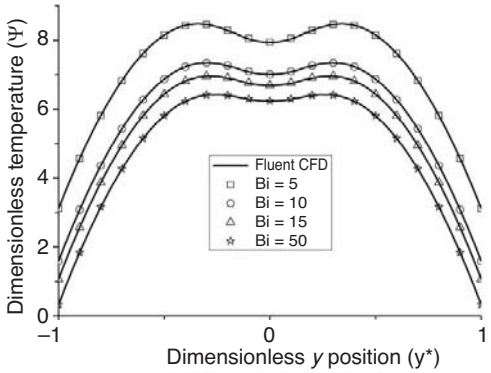

Figure 3. Variation of the dimensionless temperature along the line [AB] by dimensionless position y^* for various Biot numbers (r_o/r_i = 5, e/r_i = 2, Q = 50.0)

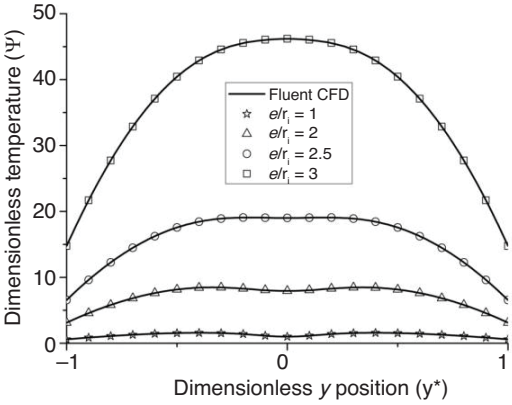

Figure 4. Variation of the dimensionless temperature through the line [AB] by dimensionless position y^* for various eccentricity ratios (r_o/r_i = 5.0)

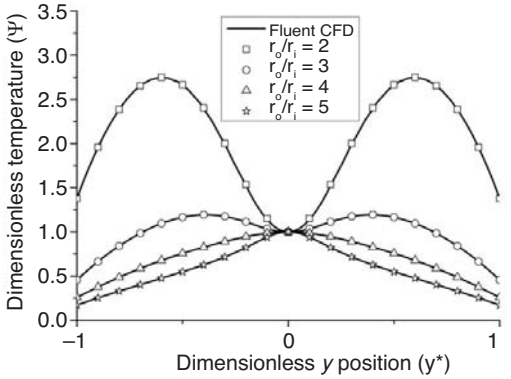

Figure 5. Variation of the dimensionless temperature through the line [CD] by dimensionless position y^* for various radii ratios (e/r_i = 0.5, Q = 50.0, Bi = 5.0)

dimensionless temperature takes the value of unity at the middle of the [CD] line as seen from the figure. For the fixed $e/r_i = 0.5$ the dimensionless eccentricities become $\delta = (e/r_i) / (r_o/r_i - 1) = 0.50$, 0.25, 0.167, and 0.125, respectively, for the radii ratios used in computations as $r_o/r_i = 2.0$, 3.0, 4.0, and 5.0, respectively. Figure 5 shows that dimensionless temperature becomes larger for larger radii ratios and consequently for larger dimensionless eccentricities.

Table 1. Dimensionless heat transfer rate $\bar{Q}$ for various eccentricities ($r_o/r_i = 5.0$)

($e/r_i = 1.0$)									
Q	–30			0			30		
Bi	CFD	BIMM	% Diff.	CFD	BIMM	% Diff.	CFD	BIMM	% Diff.
0.2	–0.651	–0.647	0.67	0.110	0.110	0.42	0.871	0.867	0.39
0.6	–1.024	–1.019	0.45	0.174	0.175	0.64	1.372	1.370	0.17
2.0	–1.280	–1.276	0.30	0.220	0.222	0.79	1.721	1.721	0.02
6.0	–1.379	–1.375	0.25	0.239	0.241	0.85	1.857	1.858	0.04
10.0	–1.400	–1.397	0.23	0.244	0.246	0.86	1.888	1.888	0.05
15.0	–1.411	–1.408	0.23	0.246	0.248	0.87	1.903	1.904	0.06
($e/r_i = 2.0$)									
Q	–30			0			30		
Bi	CFD	BIMM	% Diff.	CFD	BIMM	% Diff.	CFD	BIMM	% Diff.
0.2	–4.255	–4.240	0.34	0.107	0.108	0.32	4.470	4.456	0.31
0.6	–6.564	–6.552	0.19	0.171	0.171	0.47	6.906	6.895	0.16
2.0	–8.123	–8.115	0.09	0.221	0.222	0.58	8.564	8.559	0.06
6.0	–8.725	–8.721	0.06	0.245	0.246	0.63	9.214	9.213	0.02
10.0	–8.858	–8.854	0.05	0.251	0.252	0.65	9.360	9.359	0.01
15.0	–8.927	–8.923	0.04	0.254	0.255	0.65	9.435	9.434	0.01
($e/r_i = 3.0$)									
Q	–30			0			30		
Bi	CFD	BIMM	% Diff.	CFD	BIMM	% Diff.	CFD	BIMM	% Diff.
0.2	–21.661	–21.604	0.26	0.102	0.102	0.24	21.866	21.809	0.26
0.6	–32.232	–32.198	0.10	0.162	0.162	0.38	32.555	32.523	0.10
2.0	–39.053	–39.050	0.01	0.218	0.219	0.47	39.490	39.488	0.00
6.0	–41.700	–41.711	0.03	0.255	0.257	0.51	42.211	42.224	0.03
10.0	–42.296	–42.311	0.04	0.267	0.268	0.52	42.830	42.848	0.04
15.0	–42.605	–42.623	0.04	0.274	0.275	0.52	43.152	43.174	0.05

Heat transfer rate

In this part, the dimensionless heat transfer rates calculated using eq. (18) for different cases are compared with the Fluent CFD results. It could be noticed from eq. (20) that $h_\ell^m(\xi_o) = 0$ for uniform heat generation rate. Hence, the dimensionless heat transfer rate given by eq. (18) takes the form:

$$\bar{Q} = \frac{1}{\sqrt{2\pi}} \sum_{\ell=0}^{\infty} \sqrt{2\ell+1}\, e^{-(\ell+1/2)\xi_o} \phi_{\ell,0} \tag{21}$$

where the unknown moments $\phi_{\ell,0}$ are calculated solving (14)-(16) using eq. (20)

Table 1 tabulates computed dimensionless heat transfer, $\bar{Q}$, values for eccentricity ratios of e/r_i = 1.0, 2,0, and 3.0. In computations for each eccentricity ratio, radii ratio is fixed at r_o/r_i = 5.0, dimensionless heat generation rate takes values Q = –30, –15, 0, 15, 30, Biot number takes values Bi = 0.2, 0.6, 2.0, 6.0, 10, and 15. As seen from the table, results of BIMM agree very well with FLUENT results for all range of parameters investigated. The maximum absolute relative error is less than 1% and even much less than 1% in the most of the calculations. Eccentricity ratios used in BIMM computations as e/r_i = 1.0, 2.0, and 3.0 correspond to the dimensionless eccentricity values $\delta = (e/r_i) / (r_o/r_i - 1)$, = 0.25, 0.50, and 0.75, respectively. It could be noticed from the table that the dimensionless heat transfer rate for the same dimensionless heat generation rate and Biot number increases as δ is increased. This is because of formation of larger temperature gradients when δ is increased due to the reasons explained in Section *Effect of Biot number on temperature distribution*. A considerably greater change of rate of heat transfer is observed for relatively smaller Biot number values (Bi < 1) than for the larger Biot number of number values (Bi > 1). When Biot number exceeds practical limits (Bi ≥ 10) rate of change in the heat transfer rate is indiscriminable.

Conclusions

Heat conduction equation for an eccentric spherical annulus with heat generation whose inner surface is kept at a constant temperature and the outer surface is subjected to convection can be solved analytically using BIMM. Stating the problem in a dimensionless form in bispherical co-ordinate transforms it into a concentric annulus problem. Since Helmholtz equation is not separable or R-separable in bispherical co-ordinate an analytical Green's function to the conduction equation in bispherical co-ordinate for an eccentric annulus subject to boundary condition of third type (convection) is not possible. However, an analytical Green's function for the first type boundary conditions (given temperatures) on inner and outer boundaries can be obtained. Solution of the conduction equation with third type boundary condition on the outer surface could be expressed in terms of the unknown normal derivative of the outer surface temperature using the analytical Green's function obtained for the first type boundary condition. The resulting equation is a Fredholm integral equation of the second kind with separable kernel for the unknown normal derivative of the outer surface temperature. Taking moment of this integral equation leads to a set of linear equations which can readily be solved.

It is also possible to obtain an analytical Green's function for the second type boundary condition on the outer surface of the eccentric spherical annulus whose inner surface is kept at a constant temperature or subjected to the constant heat flux. Hence, the conduction equation with third type boundary condition on the outer surface can also be solved analytically using BIMM. In this case, the analytical Green's function obtained for the second type boundary condition is to be used in the method. The resulting equation for unknown outer surface temperature will again be a Fredholm integral equation of the same kind which can be solved by methods of moment.

The method has been applied to the eccentric spheres with various heat generation rates and for a wide range of Biot number and a perfect agreement has been observed when compared to the results of the CFD code FLUENT. This exemplifies the robustness of the method and its applicability to the conduction problems where an analytical solution for the

third type boundary condition are not accessible, but still Green's functions are obtainable for the first or second type boundary conditions.

References

[1] Ozisik, M. N., *Heat Conduction*, John Wiley and Sons, New York, USA, 1980
[2] Alassar, R. S., Alminshawy, B. J., Heat Conduction from Two Spheres, *AIChE J., 56* (2010), 9, pp. 2248-2256
[3] Alassar, R. S., Conduction in Eccentric Spherical Annuli, *International Journal of Heat and Mass Transfer, 54* (2011), 15-16, pp. 3796-3800
[4] Moon, P., Spencer, D. E., *Field Theory Handbook, Including Coordinate Systems, Differential Equations, and Their Solutions*, 2nd ed., Springer-Verlag, Berlin, Germany, 1988
[5] Yilmazer, A., Kocar, C., Exact Solution of the Heat Conduction Equation in Eccentric Spherical Annuli, *International Journal of Thermal Sciences, 68* (2013), June, pp.158-172
[6] Yılmazer, A., Kocar, C., A Novel Analytical Method for Heat Conduction in Convectively Cooled Eccentric Cylindrical Annuli, *International Journal of Thermal Sciences, 63* (2014), Sept., pp. 1-15
[7] ***, FLUENT 6 User's Guide, Fluent Inc., 2003.
[8] Arfken, G., *Mathematical Methods for Physicists*, 2nd ed., Academic Press, Orlando, Fla., USA, 1970
[9] Morse, P. M., Feshbach, H., *Methods of Theoretical Physics*, McGraw-Hill Book Company Inc, New York, USA, 1953, pp. 1298-1301
[10] Gongora-T, A., Ley-Koo, E., On the Evaluation of the Capacitance of Bispherical Capacitors, *Revista Mexicana de Física, 42* (1996), 4, pp. 663-674

Paper submitted: December 31, 2015
Paper revised: May 22, 2016
Paper accepted: May 23, 2016